Biosensors and Bioelectronics 68 (2015) 442–446

Contents lists available at ScienceDirect

Biosensors and Bioelectronics

journal homepage: www.elsevier.com/locate/bios

An ultrasensitive electrochemical DNA biosensor based on graphene/Au nanorod/polythionine for human papillomavirus DNA detection

Huayu Huang [a,*], Wanqiao Bai [a,b], Changxun Dong [c], Rui Guo [b], Zhihua Liu [a]

[a] Shaanxi Academy of Environmental Science, Xi'an 710061, China
[b] School of Chemistry and Chemical Engineering, Shaanxi University of Science and Technology, Xi'an 710021, China
[c] Department of Science, Nanjing Agricultural University, Nanjing 210095, China

ARTICLE INFO

Article history:
Received 28 October 2014
Received in revised form
8 January 2015
Accepted 16 January 2015
Available online 17 January 2015

Keywords:
Human papillomavirus
Graphene
Au nanorod
Electrochemical biosensor

ABSTRACT

An ultrasensitive electrochemical DNA biosensor for human papillomavirus (HPV) detection was developed by electrochemical impedance spectroscopy and differential pulse voltammetry. A capture probe was immobilized on a glassy carbon electrode modified with graphene/Au nanorod/polythionine (G/Au NR/PT). Two auxiliary probes were designed and used to long-range self-assemble DNA nanostructure. The target DNA can connect DNA structure to the capture probe on the electrode surface. $[Ru(phen)_3]^{2+}$ was selected as a redox indicator for amplifying electrochemical signal significantly. Enhanced sensitivity was obtained through combining the excellent electric conductivity of G/Au NR/PT architecture and the long-range self-assembly DNA nanostructure with the multi-signal amplification. The DNA biosensor displayed excellent performance for HPV DNA detection over the range from 1.0×10^{-13} to 1.0×10^{-10} mol/L with a detection limit of 4.03×10^{-14} mol/L. Furthermore, the proposed method can also be used for the detection of HPV DNA in human serum samples and provides a potential application of DNA detection in clinic research.

1. Introduction

Human papillomavirus (HPV) is a group of non-enveloped, double stranded DNA virus composed of more than 100 genotypes (Piro et al., 2011). 93%–100% of worldwide invasive carcinomas have been shown to be associated with a limited spectrum of HPV types, mostly HPV 16 and 18 (Zari et al., 2009). The detection of DNA sequences is of central importance to the virus and genetic detection, and early diagnosis of diseases (Wang et al., 2011a; Lu et al., 2009). Many techniques have been developed to detect DNA, such as, radiochemical, enzymatic, fluorescent, surface plasmon resonance spectroscopy and quartz crystal microbalance (Sutherland and Mulley, 1989; Peterlinz et al., 1997; Okahatz et al., 1998). Especially, to develop ultrasensitive methods for low-abundant HPV DNA detection is essential. A numerous ultrasensitive sequence-specific DNA detection methods including polymerase chain reaction (PCR) (Saiki et al., 1988), rolling circle amplification (RCA) (Christian et al., 2011; Cheng et al., 2009; Li et al., 2010), and nucleic-acid sequence-based amplification (Compton, 1991) were reported, but these methods require complex operation costly polymerase, tedious labels, and dedicated instrumentation (Chen et al., 2012). Electrochemical DNA biosensor with low-cost and simplicity can reach a high sensitivity via signal amplification. DNA biosensors were designed to detect a specific of target DNA (TD) by hybridization with complementary probes (Tosar et al., 2010; Campos-Ferreira et al., 2013). Xia investigated the hybridization of signal probes and TD, and created a supersandwich construction to achieve the detection limit of 1×10^{-13} mol/L (Xia et al., 2010). As the development of modern technology, most researches paid attention to detect DNA via long-range self-assembling DNA nanostructure (Chen et al., 2012; Chen et al., 2011b). Two auxiliary probes (AP) were used to create one-dimensional DNA nanostructure and fabricate an ultrasensitive biosensor for DNA detection.

Graphene, a single-atom-thick sheet of hexagonally arrayed sp^2-bonded carbon atoms (Allen et al., 2010), has shown great application potential biochemical sensors (Fowler et al., 2009). Electrochemical detection of HPV related sequences has been reported using oxidized graphene and polyaniline nanowires modified glassy carbon electrode (GCE) (Bo et al., 2011). A HPV DNA electrochemical biosensor was developed based on thionine-graphene nanocomposite modified gold electrode and achieved a limit of detection of 0.126 pmol/L (Zhu et al., 2012). Graphene-based composites may combine the outstanding properties of graphene with the special

* Corresponding author.
E-mail address: huayu.huang@hotmail.com (H. Huang).

http://dx.doi.org/10.1016/j.bios.2015.01.039
0956-5663/

functions of the other components. There have been many attempts to synthesize hybrid structures of graphene and Au nanoparticles (Muszynski et al., 2008; Coros et al., 2013; Chen et al., 2011a) which have been widely utilized in the fields of electrochemical biosensor (Hu et al., 2012; Du et al., 2010; Gautam and Jayatissa, 2012; Wang et al., 2011b). Au nanorods (Au NR) could exhibit the advantages of sensor devices due to their tunable and stronger Vis/NIR absorption, higher surface-enhanced Raman scattering cross-sections, and the possibility of unidirectional plasmon propagation (Xu et al., 2011). However, it is still a challenge for the combinations of Au NR onto the graphene sheets with good water-dispersibility. Our previous work reported the synthesis of well water-dispersible graphene/Au nanorod composites by one-step method (Bai et al., 2014).

In this study, we constructed an enzyme-free and label-free electrochemical biosensor based on graphene/Au nanorod/polythionine (G/Au NR/PT) modified glassy carbon electrode (GCE) for ultrasensitive detection for HPV DNA. Graphene could increase the electrode surface area and electrical conductivity, and Au NRs were used to enhance the immobilization of the probe DNA and ability for hybridization (Gupta et al., 2013). Thionine with good electron transfer ability has been widely used in sensor fields, and the nitrogen atom of the NH_2 moieties of thionine can strongly bind to the Au NRs surface (Wang et al., 2013). Polythionine films prepared by electrooxidative polymerization of thionine could enhance the sensitivity and lower the detection limit (Ahammad et al., 2011). The 34-base TD for the detection was from HPV-16 long terminal repeat sequences. Two AP were designed for the hybridization with TD via long-range self-assembly. 1,10-Phenanthrolineruthenium dichloride ($[Ru(phen)_3]^{2+}$) was selected as the electrochemical indicator. The experiment was optimized with different factors, and TD was also detected in complex human serum sample.

2. Experimental

2.1. Materials

All the oligonucleotides (listed in Fig. 1) were synthesized and purified by HPLC by Shanghai Shenggong Biotechnology Co. (Shanghai, China). $[Ru(phen)_3]^{2+}$, 6-mercapto-1-hexanol (MCH), thionine, Tris–HCl, tri(2-carboxyethyl) phosphine hydrochloride (TCEP) and disodium ethylene-diaminetetraacetic acid (Na_2EDTA) were purchased from sigma-aldrich (USA). Other chemicals were of analytical grade. Deionized water was prepared from a Milli-Q water purification system (Bedford, MA). The buffers and solutions were prepared as follows: DNA immobilization buffer (I-buffer, pH=7.4, 10 mmol/L Tris–HCl +1 mmol/L EDTA+500 mmol/L NaCl+10 mmol/L TCEP), DNA hybridization buffer (H-buffer, pH=7.4, 10 mmol/L Tris–HCl +1 mmol/L EDTA+500 mmol/L NaCl+1 mmol/L $MgCl_2$), electrochemistry buffer (E-buffer, pH=7.4, 10 mmol/L Tris–HCl), MCH solution (2 mmol/L in water), and $[Ru(phen)_3]^{2+}$ solution (pH=7.4, 5 mmol/L $[Ru(phen)_3]^{2+}$ in E-buffer).

2.2. Electrode pretreatment

The 3 mm-diameter glassy carbon electrode (GCE) was initially polished with 0.05 μm alumina slurry, and then sonicated in water for 2 min to give a clean surface. Well dispersed G/Au NRs

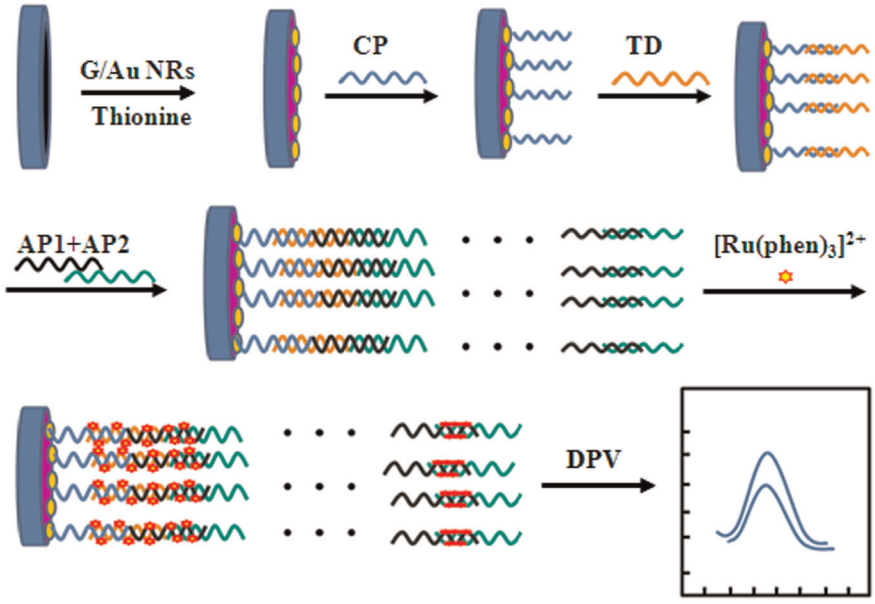

Oligonucleotide	Sequence (from 5' to 3')
capture probe (CP)	TTTCAATTTTTGGATTAC-$(CH_2)_6$-SH
complementary target DNA (TD)	GTAATCCAAAAATTGAAAACTAAGGGTCTGAGGG
auxiliary probe 1 (AP1)	TACTCCCCCAGGTGC CCCTCAGACCCTTAGT
auxiliary probe 2 (AP2)	GCACCTGGGGGAGTA ACTAAGGGTCTGAGGG
single-base mismatch target (1MT)	GTAATCCAATAATTGAAAACTAAGGGTCTGAGGG
two-base mismatch target (2MT)	GTAATCCAATTATTGAAAACTAAGGGTCTGAGGG
noncomplementary sequence (NC)	CCTTTTAGTCAGTGTGGAAATCTCTAGCAGTGGC

Fig. 1. Schematic representation of the long-range self-assembled DNA electrochemical biosensor.

composites were synthesized and characterized as our previous work (Bai et al., 2014).

5.0 μL of G/Au NRs dispersion (0.5 mg/mL) was dropped onto the surface of a GCE and dried naturally at room temperature. Thionine was then electropolymerized on the G/Au NR GCE followed the reported method (Zhang and Huang, 2012). The deposition experiment was carried out from an acetate buffer solution (0.1 mol/L, pH=6.0) containing 0.5 mmol/L thionine using cyclic voltammetry (CV). The electrode potential was cycled from −0.4 mV to 0.1 mV for 15 cycles at 50 mV/s scan rate. After the electrodeposition, the G/Au NR/PT modified electrode was dried in air.

2.3. DNA self-assembly

The electrodeposited GCE was incubated in 6 μL of I-buffer containing 1 μmol/L thiolated capture probes (CP) for 3 h, rinsed with deionized water and then dried under nitrogen gas environment. After the electrode was incubated in 1.0 μmol/L MCH solution for 90 min to remove nonspecific DNA adsorption, it was washed and dried in nitrogen again. 6 μL of target DNA (1.0 μmol/L in H-buffer) was pipetted to the modified GCE surface and incubated for 90 min. The modified GCE was also rinsed and dried. Then, 10 μL of H-buffer containing AP1 and AP2 was dropped on the electrode surface and incubated for 90 min to complete the self-assembly. Finally, the desirable electrode self-assembled with DNA was rinsed and dried in nitrogen for further electrochemical detection.

2.4. Detection procedure

Electrochemical measurements were performed with a CHI 600D electrochemical workstation (Shanghai Chenhua Instrument Co. Ltd., China) with a conventional three-electrode system. The working electrode is a modified GCE, the reference electrode is a Ag/AgCl electrode, and the counter electrode is a platinum wire.

The biosensor was characterized by electrochemical impedance spectroscopy (EIS) in 0.02 mol/L phosphate buffer solution (PBS) containing 5 mmol/L $[Fe(CN)_6]^{3-/4-}$ at perturbation amplitude of 0.1 V within the frequency range of 0.1 Hz–0.1 MHz. Differential pulse voltammetry (DPV) was recorded from −0.6 to 0.1 V in 3 mL $[Ru(phen)_3]^{2+}$ solution degassed with nitrogen for 15 min. The pulse amplitude was 50 mV, and the pulse width was 0.05 s.

3. Results and discussion

3.1. Design of electrochemical biosensor

The fabrication of the biosensor and detection of DNA is shown in Fig. 1. G/Au NRs were first deposited onto the bare GCE and then thionine was electropolymerized on G/Au NRs film. G/Au NR/PT modified GCE provided an excellent platform for further immobilization. CP was immobilized on G/Au NR/PT GCE both through strong Au–S bond (Zhang et al., 2014; Zhang and Huang, 2012), and the electrostatic interaction with the positively charge Au NRs (Lu et al., 2013). The presence of MCH aimed to block the nonspecific binding sites. Subsequently, one terminal of TD was immobilized on the electrode via hybridizing with CP, and the other terminal of TD hybridized with AP1. AP2 was introduced to hybridize with AP1. The liberated target triggered the connection of a long DNA nanostructure to CP. Numerous $[Ru(phen)_3]^{2+}$ were bound to the DNA nanostructure with negative charges via electrostatic interaction and enhanced significantly electrochemical signals.

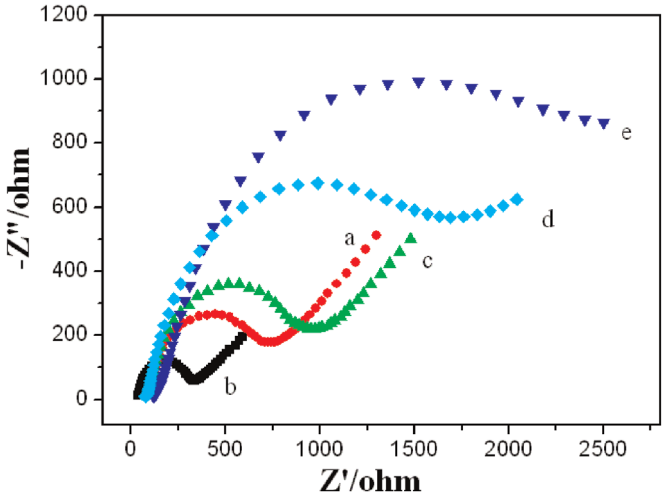

Fig. 2. EIS at bare GCE (a), G/Au NR/PT GCE (b), G/Au NR/PT/CP GCE (c), G/Au NR/PT/CP/TD GCE (d) and G/Au NR/PT/CP/TD/AP GCE (e) in 0.02 mol/L PBS solution containing 5 mmol/L $[Fe(CN)_6]^{3-/4-}$.

3.2. Electrochemical characterization

EIS was an effective technique to investigate the changes of the electrode behavior after each assembly step. The impedance of spectra included a semicircle portion at higher frequencies corresponding to the electro-transfer resistance (R_{et}) and a linear portion at lower frequencies representing the diffusion process. Fig. 2 exhibits the Nyquist plots at bare GCE, G/Au NR/PT GCE, G/Au NR/PT/CP GCE, G/Au NR/PT/CP/TD GCE and G/Au NR/PT/CP/TD/AP GCE. The bare GCE displayed a semicircle with a R_{et} of about 725 Ω. The electrode modified with G/Au NR/PT composite film showed a much lower resistance (330 Ω), which indicated that G/Au NR/PT was an excellent electric conducting material and accelerated the electron transfer. The R_{et} increased evidently (970 Ω) because CP loaded on the surface of G/Au NR/PT modified electrode formed an additional barrier and further prevented the redox probe to the electrode surface. Enhancement R_{et} (1670 Ω) is found after hybridization of TD with CP as a result of increase in the negative charge owing to double-stranded DNA formation. Furthermore, the R_{et} reached to about 2515 Ω after self-assembled with AP, which indicated the formation of complex layer embarrassing the electrode transfer.

$[Ru(phen)_3]^{2+}$ was utilized as the electrochemical indicator. The bindings of $[Ru(phen)_3]^{2+}$ to the phosphate backbone of DNA were completely through electrostatic interaction. The redox charge of $[Ru(phen)_3]^{2+}$ was a direct function of the amounts of DNA localized on electrode surfaces. Fig. 3 shows DPV responses of GCE modified with various oligonucleotides. CP was immobilized on the electrode surface via gold–thiol bindings. A weak oxidation peak can be observed in the absence of TD, because there were a few of $[Ru(phen)_3]^{2+}$ binding to CP. More $[Ru(phen)_3]^{2+}$ cations were binding to CP and TD, and the electrochemical response was slightly higher under the existence of TD. AP1 and AP2 can self-assemble to be DNA nanostructure and can not link to the electrode surface without TD. From Fig. 3, it can be seen that there was still a small oxidation peak in the presence of TD and AP1. The electrochemical response enhanced significantly owing to a great number of $[Ru(phen)_3]^{2+}$ binding to DNA nanostructure, after AP1 and AP2 were immobilized on the electrode surface via TD and CP.

3.3. Optimization of self-assembled DNA

Fig. S1 shows the effects of accumulation time on the oxidation peak current. The peak current increased greatly as the

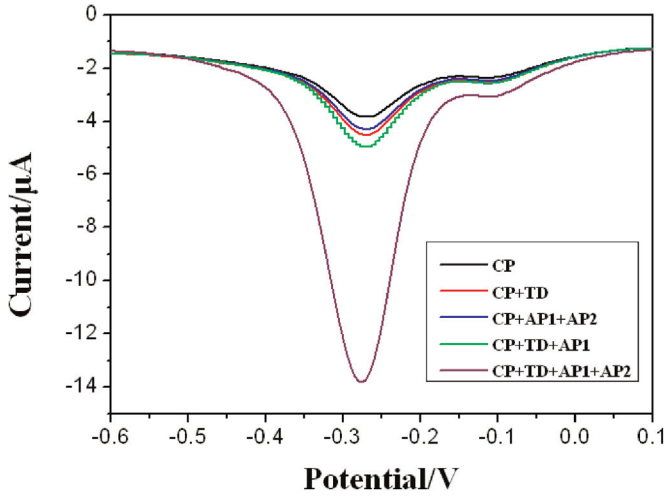

Fig. 3. DPV response of GCE modified with various oligonucleotides. The concentration of TD is 1.0×10^{-10} mol/L and the concentration of AP1 and AP2 are both 1.0×10^{-6} mol/L.

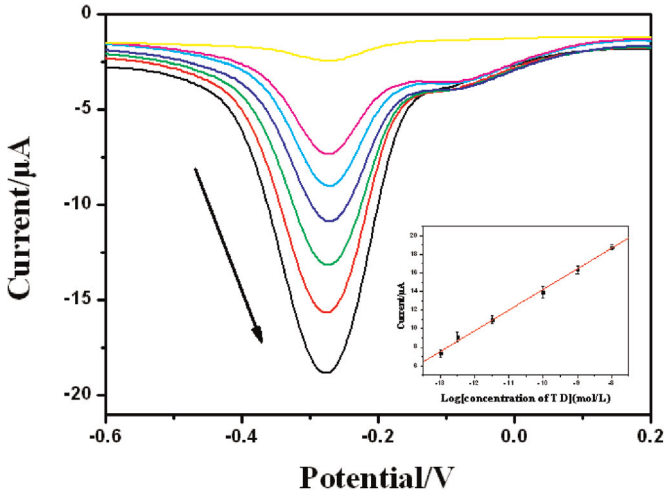

Fig. 4. DPV responses for different concentrations of TD (1.0×10^{-13}, 3.0×10^{-13}, 3.0×10^{-12}, 1.0×10^{-10}, 1.0×10^{-9} and 1.0×10^{-8} mol/L).

accumulation time increased from 0 to 6 min and decreased slightly after 6 min, because the nonspecific adsorption increased after the specific adsorption was saturated. From the perspective of sensitivity, 6-min accumulation was selected in this work. The effects of thionine concentration on the oxidation peak current were investigated and shown in Fig. S2. The oxidation peak current increased with increasing thionine concentration from 0 to 1.0 mmol/L. The phenomenon revealed that it was efficient for thionine to improve the detection sensitivity. The oxidation peak response remained a relative constant with improving thionine concentration from 0.5 to 1.0 mmol/L, so 0.5 mmol/L of thionine was employed owing to consider sensitivity and analytical cost. The effects of the concentration of AP1 and AP2 a on the oxidation peak current were studied. Fig. S3 shows effects of the concentration of AP1 and AP2 for detection TD. AP1 and AP2 were both the same concentration. It can be seen that the electrochemical response increased with increasing the concentration up to 1.0 mol/L and tended to a steady value from 1.0 to 2.0 μmol/L. The optimal concentration of AP was 1.0 μmol/L. The effects of hybridization time on the electrochemical signal were also investigated (Fig. S4). The signal increased dramatically with the hybridization time from 0 to 90 min and then remained nearly constant. Therefore, 90 min was selected as the optimized hybridization time.

3.4. Electrochemical detection of TD

The linear range and detection limit of TD were tested with DPV under the optimized conditions. As shown in Fig. 4, it was found that the DPV peak current increased with increasing the concentration of TD. The inset showed the good linear relationship between the peak current (i_p, A) and the logarithm of TD concentration (C, mol/L) over the range from 1.0×10^{-8} to 1.0×10^{-13} mol/L. The linear regression equation is $i_p = 2.2212 \times \lg C + 36.4478$, and the correlation coefficient is 0.9986. The detection limit was evaluated to be 4.03×10^{-14} mol/L based on three signal-to-noise ratio. For comparison, the HPV DNA detection with G/Au NR/PT modified GCE and the previous published electrochemical methods were listed in Table 1. It can be seen that the present method achieved a broader linear range and a lower detection limit for HPV DNA detection than other methods. Hence, G/Au NR/PT modified GCE was confirmed to be an efficient platform for the electrochemical sensor. The obtained ultrasensitivity can be explained by two reasons (Chen et al., 2012). On one hand, the significant length of the self-assembled DNA nanostructure enhanced the electrochemical responses. On the other hand, DNA nanostructures with biocompatibility and hydrophilicity were less prone to nonspecific adsorption onto the electrode surface.

3.5. Selectivity of the biosensor

In order to investigate the selectivity of the biosensor, four kinds of DNA sequences were chosen to compare, including TD, single-base mismatch target (1MT), two-base mismatch target (2MT), and noncomplementary sequence (NC). Fig. 5 shows the peak current of the blank and the four kinds of DNA sequences. The concentration of TD was 1.0×10^{-12} mol/L, and the concentration of other DNA sequences was 1.0×10^{-9} mol/L. Although the concentration of the disrupting DNA was higher than that of TD, the DPV signal of 1MT was approximately one third of TD signal. It can be explained that the non-complementary DNA could not be hybridized with CP and the response of the mismatch DNA was induced by the non-specific hybridization. The results revealed that the biosensing platform could be used to detect HPV with high specificity and ultrasensitivity.

3.6. Interference

TD was detected in human serum in order to evaluate the performance of the method in complex condition. The examination was performed by standard addition method. TD sample with known concentration was prepared with human serum. Fig. S5 shows the comparison of the peak currents in H-buffer and human serum under the same experimental condition. The DPV signal was decreased a little in complex serum sample due to the interference of the sample matrix during the hybridization between TD and CP. However, DPV response of the blank was higher in the serum than in H-buffer, which meant that the existence of the nonspecific adsorption from the components in biological sample. From Fig. S5, it can be seen that a lower concentration of TD (6.0×10^{-12} mol/L) was still detected in human serum. The results indicated the feasibility of the prepared biosensor in real physiological media.

4. Conclusions

An ultrasensitive electrochemical DNA biosensor was developed for specific detection of HPV DNA based on G/Au NR/PT

Table 1
Comparison of the detection limits and linear ranges of different electrochemical biosensors for HPV DNA.

Modified material and electrode	Detection technique	Linear range (nmol/L)	Detection limit (nmol/L)	Reference
L-Cysteine gold electrode	DPV	18.75–250	18.13	Campos-Ferreira et al. (2013)
Pyrrolidinyl peptide nucleic acid carbon electrode	SWV	20–1.2×10^{4}	4.0	Jampasa et al. (2014)
Brilliant cresyl blue carbon past electrode	DPV	10–5000	9.0	Hejazi et al. (2010)
Polyaniline/MWCNT platinum electrode	SWV	10–50	0.49	Tran et al. (2011)
Graphene/polyaniline nanowires glassy carbon electrode	CV	2.12×10^{-3}–2120	3.25×10^{-4}	Bo et al. (2011)
Thionine/grapheme gold electrode	DPV	1×10^{-3}–100	1.26×10^{-4}	Zhu et al. (2012)
Graphene/gold nanorod/polythionine glassy carbon electrode	DPV	1×10^{-4}–10	4.03×10^{-5}	This work

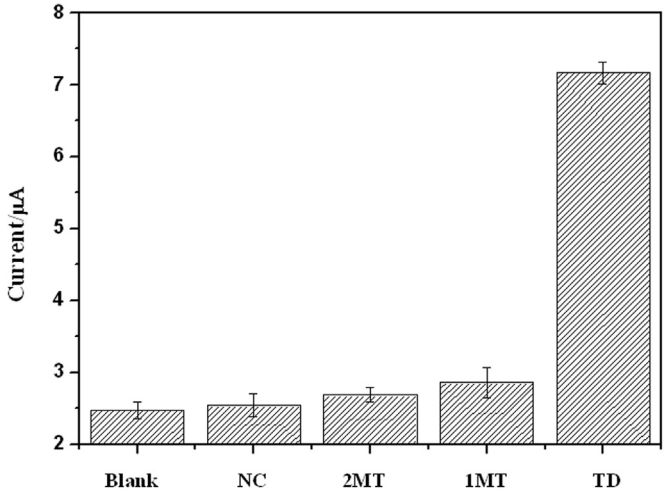

Fig. 5. Comparison of DPV responses of the blank and the four different DNA sequences. (Single-base mismatch target: 1MT; two-base mismatch target: 2MT; noncomplementary sequence: NC).

composites. The signal amplification was carried out via a long-range self-assembled DNA nanostructure. The proposed biosensor demonstrated good selectivity and remarkable detection limit. HPV DNA was also can be detected in human serum with the present method. The designed DNA biosensor without any enzyme and label has a great potential in HPV DNA diagnostics and clinical analysis.

Acknowledgments

This work was supported by the Shaanxi Province Ke Ji Tong Chou Chuang Xin project (2011KTZB03-03-01-02).

Appendix A. Supplementary material

Supplementary data associated with this article can be found in the online version at http://dx.doi.org/10.1016/j.bios.2015.01.039.

References

Ahammad, A.J.S., Rahman, M.M., Xu, G.-R., Kim, S., Lee, J.-J., 2011. Electrochim. Acta 56, 5266–5271.
Allen, M.J., Tung, V.C., Kaner, R.B., 2010. Chem. Rev. 110, 132–145.
Bai, W., Huang, H., Li, Y., Zhang, H., Liang, B., Guo, R., Du, L., Zhang, Z., 2014. Electrochim. Acta 117, 322–328.
Bo, Y., Yang, H., Hu, Y., Yao, T., Huang, S., 2011. Electrochim. Acta 56, 2676–2681.
Campos-Ferreira, D.S., Nascimento, G.A., Souza, E.V.M., Souto-Maior, M.A., Arruda, M.S., Zanforlin, D.M.L., Ekert, M.H.F., Bruneska, D., Lima-Filho, J.L., 2013. Anal. Chim. Acta 804, 258–263.
Chen, X., Hong, C.-Y., Lin, Y.-H., Chen, J.-H., Chen, G.-N., Yang, H.-H., 2012. Anal. Chem. 84, 8277–8283.
Chen, Y., Li, Y., Sun, D., Tian, D.B., Zhang, J.R., Zhu, J.J., 2011a. J. Mater. Chem. 21, 7604–7611.
Chen, X., Lin, Y.-H., Li, J., Lin, L.-S., Chen, G.-N., Yang, H.-H., 2011b. Chem. Commun. 47, 12116–12118.
Cheng, Y.Q., Zhang, X., Li, Z.P., Jiao, X.X., Wang, Y.C., Zhang, Y.L., 2009. Angew. Chem. Int. Ed. 48, 3268–3272.
Christian, A.T., Pattee, M.S., Attix, C.M., Reed, B.E., Sorensen, K.J., Tucker, J.D., 2011. Proc. Natl. Acad. Sci. U. S. A. 98, 14238–14243.
Compton, J., 1991. Nature 350, 91–92.
Coros, M., Biris, A.R., Pogacean, F., Tudoran, L.B., Neamtu, C., Watanabe, F., Birisc, A. S., Pruneanu, S., 2013. Electrochim. Acta 91, 137–143.
Du, M., Yang, T., Jiao, K., 2010. J. Mater. Chem 20, 9253–9260.
Fowler, J.D., Allen, M.J., Tung, V.C., Yang, Y., Kaner, R.B., Weiller, B.H., 2009. ACS Nano 3, 206–301.
Gautam, M., Jayatissa, A.H., 2012. Solid State Electron. 78, 159–165.
Gupta, V., Yola, M., Qureshi, M.S., Solak, A.O., Atar, N., Üstündağ, Z., 2013. Sens. Actuators B Chem. 188, 1201–1211.
Hejazi, M.S., Raoof, J.B., Ojani, R., Golabi, S.M., Asl, E.H., 2010. Bioelectrochemistry 78, 141–146.
Hu, S., Wang, Y.H., Wang, X.Z., Xu, L., Xiang, J., Sun, W., 2012. Sens. Actuators B Chem. 168, 27–33.
Jampasa, S., Wonsawat, W., Rodthongkum, N., Siangproh, W., Yanatatsaneejit, P., Vilaivan, T., Chailapakul, O., 2014. Biosens. Bioelectron. 54, 428–434.
Li, J.S., Deng, T., Chu, X., Yang, R.H., Jiang, J.H., Shen, G.L., Yu, R.Q., 2010. Anal. Chem. 82, 2811–2816.
Lu, C.H., Yang, H.H., Zhu, C.L., Chen, X., Chen, G.N., 2009. Angew. Chem. Int. Ed. 48, 4785–4787.
Lu, X., Dong, X., Zhang, K., Han, X., Fang, X., Zhang, Y., 2013. Analyst 138, 642–650.
Muszynski, R., Seger, B., Kamat, P.V., 2008. J. Phys. Chem. C 112, 5263–5266.
Okahatz, Y., Kawase, M., Niikura, K., Ohtake, F., Furasawa, H., Ebara, Y., 1998. Anal. Chem. 70, 1288–1296.
Peterlinz, K.A., Georgiadis, R.M., Herne, T.M., Tarlov, M.J., 1997. J. Am. Chem. Soc. 119, 3401–3402.
Piro, B., Kapella, A., Le, V.H., Anquetin, G., Zhang, Q.D., Reisberg, S., Noel, V., Tran, L. D., Duc, H.T., Pham, M.C., 2011. Electrochim. Acta 56, 10688–10693.
Saiki, R.K., Gelfand, D.H., Stoffel, S., Scharf, S.J., Higuchi, R., Horn, G.T., Mullis, K.B., Erlich, H.A., 1988. Science 239, 487–491.
Sutherland, G., Mulley, J., 1989. In: Symons, R.H. (Ed.), Nucleic Acid Probes. CRC Press, Boca Raton, FL, p. 159.
Tosar, J.P., Braňas, G., Laíz, J., 2010. Biosens. Bioelectron. 26, 1205–1217.
Tran, L.D., Nguyen, D.T., Nguyen, B.H., Do, Q.P., Nguyen, H.L., 2011. Talanta 85, 1560–1565.
Wang, C.S., Li, J.Y., Amatore, C., Chen, Y., Jiang, H., Wang, X.M., 2011a. Angew. Chem. Int. Ed. 50, 11644–11648.
Wang, F., Elbaz, J., Orbach, R., Magen, N., Willner, I., 2011b. J. Am. Chem. Soc. 133, 17149–17151.
Wang, W., Song, L., Gao, Q., Qi, H., Zhang, C., 2013. Electrochem. Commun. 34, 18–21.
Xia, F., White, R.J., Zuo, X.L., Patterson, A., Xiao, Y., Kang, D., Gong, X., Plaxco, K.W., Heeger, A.J., 2010. J. Am. Chem. Soc. 132, 14346–14348.
Xu, L.G., Kuang, H., Wang, L.B., Xu, C.L., 2011. J. Mater. Chem. 21, 16759–16782.
Zari, N., Amine, A., Ennaji, M.M., 2009. Anal. Lett. 42, 519–535.
Zhang, P., Wu, X., Chai, Y., Yuan, R., 2014. Analyst 139, 2748–2753.
Zhang, Y., Huang, L., 2012. Microchim. Acta 176, 463–470.
Zhu, L., Luo, L., Wang, Z., 2012. Biosens. Bioelectron. 35, 507–511.